Journal of Hazardous Materials Advances 12 (2023) 100380

Contents lists available at ScienceDirect

Journal of Hazardous Materials Advances

journal homepage: www.elsevier.com/locate/hazadv

Insights into the dopant engineering in copper-doped $SrTiO_3$ nanocubes

D. Krishna Bhat [a,*], Uma PI [a], U. Sandhya Shenoy [b,*]

[a] Department of Chemistry, National Institute of Technology Karnataka, Surathkal, Mangalore 575025, India
[b] Department of Materials Science and Engineering, Institute of Engineering and Technology, Srinivas University, Mukka, Mangalore 574146, India

ARTICLE INFO

Keywords:
Strontium titanate
Dye degradation
Electronic structure
Photocatalysis
Doping

ABSTRACT

In recent years, semiconductors have captivated the scientific community due to their potential to harness the abundant and sustainable energy from the sun to effectively treat water pollutants. Herein, we present combined theoretical and experimental insights into the enhanced activity of photocatalytic degradation of cationic and anionic dye viz methylene blue (100% in 90 min) and rose bengal (99.6% in 30 min) in presence of copper doped $SrTiO_3$ catalyst. First principles density functional theory study reveals the introduction of additional states due to copper doping resulting in the decrease in the band gap making it visible light active. Experimental analysis reveals a change in the morphology from broccoli type assorted spherical particles to cubic shaped structures resulting in three times increase in the surface area as a consequence of doping copper. The adopted one pot solvothermal approach not only resulted in materials with high cyclic stability but also resulted in a versatile material, which can be applied for degradation of other dyes.

Introduction

The ever-increasing world population has raised the usage of textile dyes, which are harming the environment in an irreversible manner by contaminating the soil and water bodies causing serious health hazards for humans and other living organisms (Uma et al., 2023). Although there are several techniques developed for the removal of contaminants, it is taxing to remove these dyes from water resources as they are non-biodegradable and water soluble (Alimohammadi et al., 2023). Metal oxides with general formula ABO_3 with perovskite structures are widely investigated for their various activities due to their compositional flexibility and robust crystalline structure (Uma et al., 2023; Zhang et al., 2023; Bhat et al., 2020; Shenoy and Bhat, 2020). Strontium titanate ($SrTiO_3$), an alkaline earth titanate is a proven photocatalyst under UV light but is unsuitable for visible light photocatalysis due to its wide bandgap (Song et al., 2021; Merrad et al., 2022; Bantawal et al., 2018; Nunocha et al., 2022). Since, visible light occupies the major portion of solar radiation reaching earth, visible light active photocatalysts to eliminate the waste dyes from the ecosystem are highly sort after (Sadiq et al., 2018; Mohamed et al., 2018). Substitutional doping can be used to introduce any foreign cation from the periodic table in the A and B sites of the ABO_3 crystal lattice which results in introduction of additional energy states (Xu et al., 2023; Shenoy and Bhat, 2021). The formation of dopant states between the valence and conduction bands of the semiconductor decreases the band gap enabling the absorption of light in the visible region (Shenoy and Bhat, 2020). Doping of Ag, Al, Cd, Cu, Eu, Fe, La, Mn, Nb, Ni, Rh, V was earlier reported to cause changes in the properties of $SrTiO_3$ by altering the electronic structure making it a better photocatalyst than the undoped one (Ordoñez et al., 2023; Chu et al., 2022; Kafeshani et al., 2022; Rahman et al., 2012; Jang et al., 2021; Wang et al., 2023; Nunocha et al., 2021; Paul et al., 2023; Zhu et al., 2022; Shenoy et al., 2018; Bantawal et al., 2020). Yet the activities of these materials in degradation of dyes like methylene blue (MB) and rose bengal (RB) is not upto the desired level (Shenoy et al., 2018; Bantawal et al., 2020; Rosy and Kalpana, 2018). This is due to the introduction of mid gap states which acts as recombination centres created as a result of doping in specific lattice sites (Shenoy et al., 2018). The crystal and electronic structure tunability of $SrTiO_3$ is exploited in this work by doping copper. The unique result of doping copper is that irrespective of the site the dopant occupies mid gap recombination centres are not created. This is highly beneficial because directed synthesis is not essential as in the case of other dopants (Bhat et al., 2020; Shenoy et al., 2018). To overcome the drawbacks of previously reported sol gel technique which resulted in low photocatalytic efficiency we employed a simple solvothermal route for synthesis of Cu doped $SrTiO_3$ (Rahman et al., 2012). High photocatalytic degradation activity of 99.6% RB within 30 min and nearly 100% of MB in 90 min was achieved in the present work.

* Corresponding authors.
E-mail addresses: denthajekb@gmail.com (D.K. Bhat), sandhyashenoy347@gmail.com (U.S. Shenoy).

https://doi.org/10.1016/j.hazadv.2023.100380
Received 15 July 2023; Received in revised form 3 October 2023; Accepted 5 October 2023
Available online 7 October 2023

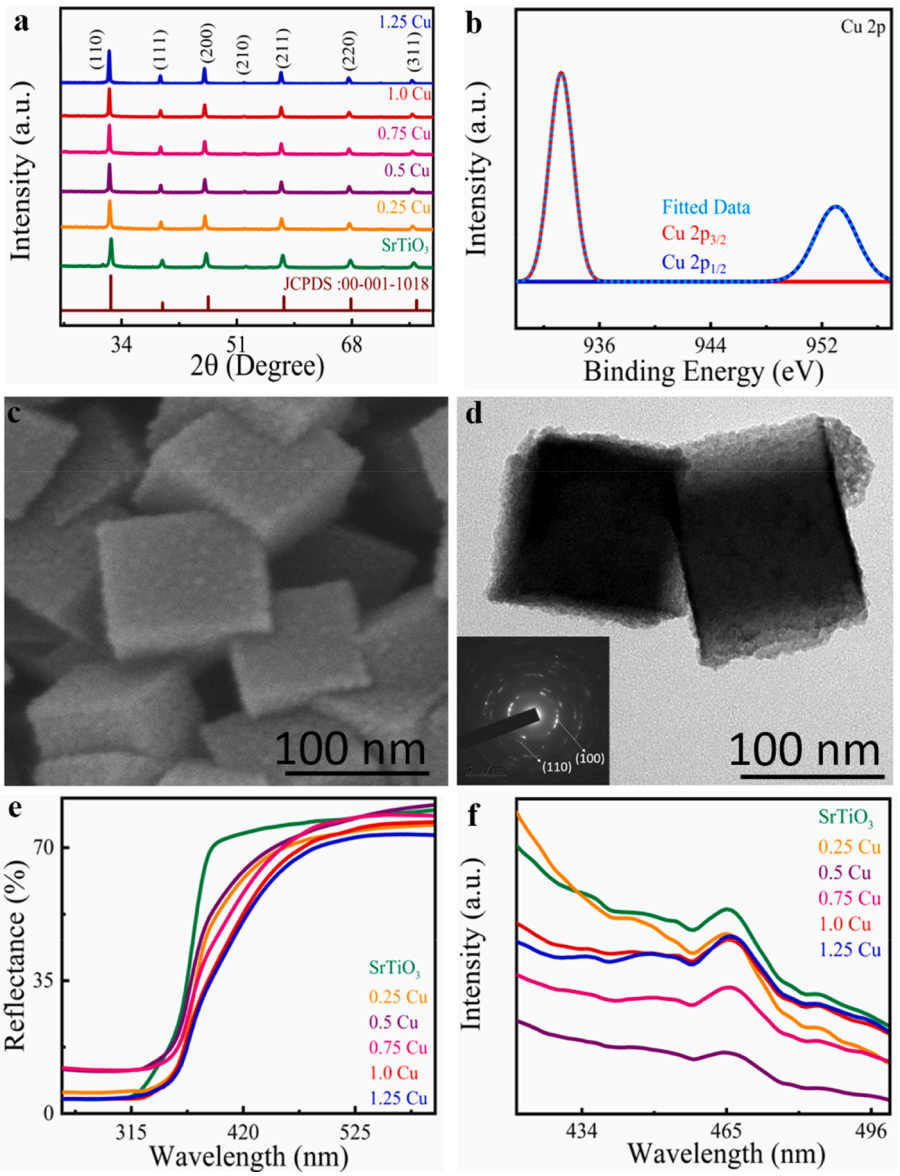

Fig. 1. (a) XRD patterns of undoped and doped $SrTiO_3$, (b) Cu 2p XPS plot of 0.5 Cu, (c) FESEM image of 0.5 Cu, (d) TEM image of 0.5 Cu (Inset shows SAED pattern), (e) UV–visible DR spectra, (f) PL spectra of all samples.

Methods

Synthesis

All the chemicals were purchased from Sigma Aldrich and used without purification. Doped and undoped perovskites are prepared via a one-pot solvothermal method (Uma et al., 2023). About 1.5 mL of titanium isopropoxide was dissolved in 10 mL of isopropanol. A calculated amount of copper acetate monohydrate was added to the mixture and stirred well. The Ti and Sr precursors are taken in a 1:1 molar ratio. Then strontium nitrate was added and magnetically stirred for 30 min to attain complete dissolution. 15 mL of 5 M KOH solution was added dropwise and the whole reaction mixture was allowed to stir for 1 h. The resultant mixture was autoclaved at 200 °C for 4 h. The precipitate formed was washed with acetic acid and distilled water to remove the impurities. The product was finally obtained by drying it in a hot air oven at 50 °C overnight. Similarly, the undoped $SrTiO_3$ was synthesized without adding the copper precursor. Thus, the samples prepared were marked as $SrTiO_3$, 0.25 Cu, 0.5 Cu, 0.75 Cu, 1.0 Cu and 1.25 Cu when 0 mol%, 0.25 mol%, 0.5 mol%, 0.75 mol%, 1.0 mol% and 1.25 mol% of copper precursor were used. The details of the characterization techniques and photocatalytic experiments are provided in the supplementary information.

Computational technique

We used quantum ESPRESSO package built within the framework of density functional theory (DFT) to study the electronic structure of $SrTiO_3$ and copper doped $SrTiO_3$ (Giannozzi et al., 2009). Ultrasoft pseudopotentials with Perdew, Burke and Ernzerhof exchange correlation functional for electrons was chosen (Perdew et al., 1996). In our calculations we considered a plane wave basis set with cutoff of 50 Ry for energy and 400 Ry for charge density values. $SrTiO_3$ represents the most typical perovskite oxide with a cubic structure formed by Sr atoms at the corner, Ti at the centre and O occupying the face centres (Shenoy et al., 2018). The doped configurations were simulated using a $3 \times 3 \times 3$ supercell of cubic $SrTiO_3$ structure by substituting either Sr atom or Ti atom with Cu atom. A fully relaxed structure with respect to the lattice parameters and atomic positions were chosen for the calculation of total energies. A $3 \times 3 \times 3$ and $6 \times 6 \times 6$ mesh of k points was used for scf and

Table 1
XPS binding energy data of elements in 0.5 Cu nanocubes.

Elements	Spin state/type	Binding energy (eV)	Oxidation state	Refs.
Sr	$3d_{5/2}$	133.68	+2	Cheng et al. (2022)
	$3d_{3/2}$	135.38		
Ti	$2p_{3/2}$	459.29	+4	Sohrabian et al. (2023)
	$2p_{1/2}$	465.03		
O	Lattice (O_L)	530.65	–	Bantawal et al. (2021)
	Hydroxyl oxygen (O_{OH})	532.35		
Cu	$2p_{3/2}$	933.27	+2	More et al. (2022)
	$2p_{1/2}$	952.94		

nscf calculations. Γ - X - M - Γ - R - X high symmetry path was chosen for the determination of electronic structure.

Results and discussion

The X-ray diffraction (XRD) patterns of synthesized $SrTiO_3$ and Cu doped $SrTiO_3$ match well with the standard perovskite phase of $SrTiO_3$ (JCPDS card no. 00-001-1018). Cu as a dopant can either occupy the lattice site or enter into the interstitial site depending on the host material and synthetic technique applied (Uma et al., 2023; Kihoi et al., 2022; Kim et al., 2023). The inclusion of Cu^{2+} into the Ti^{4+} site in the present case was evident from the shift in the 2θ to lower values for the doped samples (Fig. 1a) (Uma et al., 2023). The decrease in 2θ value was due to the substitution of a larger cation (Cu^{2+}: 73 Å) in the place of a smaller cation site (Ti^{4+}: 60.5 Å) causing lattice expansion, increasing the lattice parameter and hence decreasing the 2θ value (Uma et al., 2023). The qualitative identification of components like Sr, Ti, O, and Cu was carried out using the X-ray photoelectron spectroscopy (XPS) analysis (Figs. S1 and S2). The high resolution XPS spectrum of Cu 2p indicates the successful incorporation of Cu in the 0.5 Cu nanocubes (Fig. 1b). The binding energy values and corresponding oxidation states of the elements present in the 0.5 Cu sample are given in Table 1.

The field emission scanning electron microscopy (FESEM) and transmission electron microscopy (TEM) images of $SrTiO_3$ showed broccoli-like assemblage and clustered spherical nanoparticles respectively (Fig. S3). (Bantawal et al., 2019) The Cu doping altered the morphology of the $SrTiO_3$ sample into a cubic structure as evident from the FESEM and TEM images of the 0.5 Cu sample (Fig. 1c and d). The growth in the direction of ⟨100⟩ due to Cu doping resulted in the formation of nanocubes (HRTEM image, Fig. S4). (Sun and Xia, 2002) From the Brunauer–Emmett–Teller (BET) isotherm results, a type IV adsorption pattern with H3 hysteresis loop was observed (Fig. S5) (Bhat et al., 2023). The surface area of the 0.5 Cu naocubes (91.98 $m^2\ g^{-1}$) was found three times greater than $SrTiO_3$ (30.46 $m^2\ g^{-1}$). Spherical particles have the lowest surface area for a given volume. The undoped $SrTiO_3$ consisted of clustered spherical particles which further resulted in decrease of its surface area due to the agglomeration. Cube shaped particles have higher surface area than spherical particles for a given volume. Hence, we observed that doping results in the increase in the surface area of the photocatalyst due to change in its morphology. The high value of the surface area of the doped sample propounds the greater availability of the photocatalyst surface for the dye molecule to adhere. As is known, in any catalytical process, adsorption is an essential step. The adsorption of the dye molecules leads to greater contact of the catalyst with the dye molecules leading to effective reaction with the

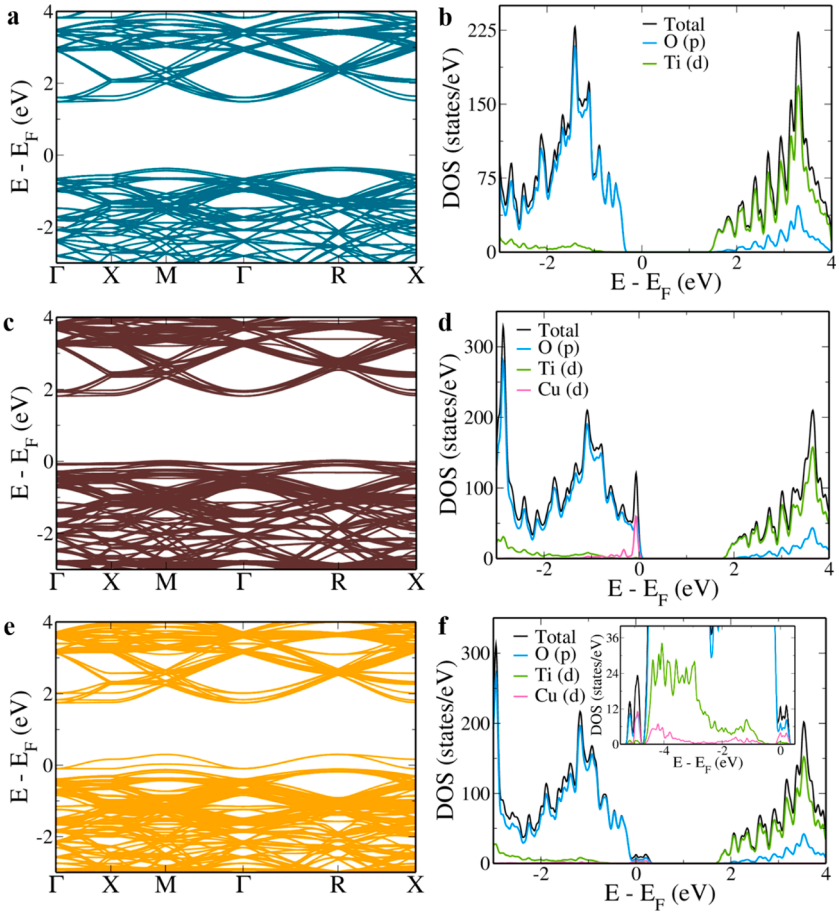

Fig. 2. Electronic structure and pDOS of (a and b) $SrTiO_3$, Cu doped $SrTiO_3$ with (c and d) Cu in Sr site, (e and f) Cu in Ti site (Inset shows pDOS at larger range of energy). The energy is shifted with respect to the Fermi level which is set to zero.

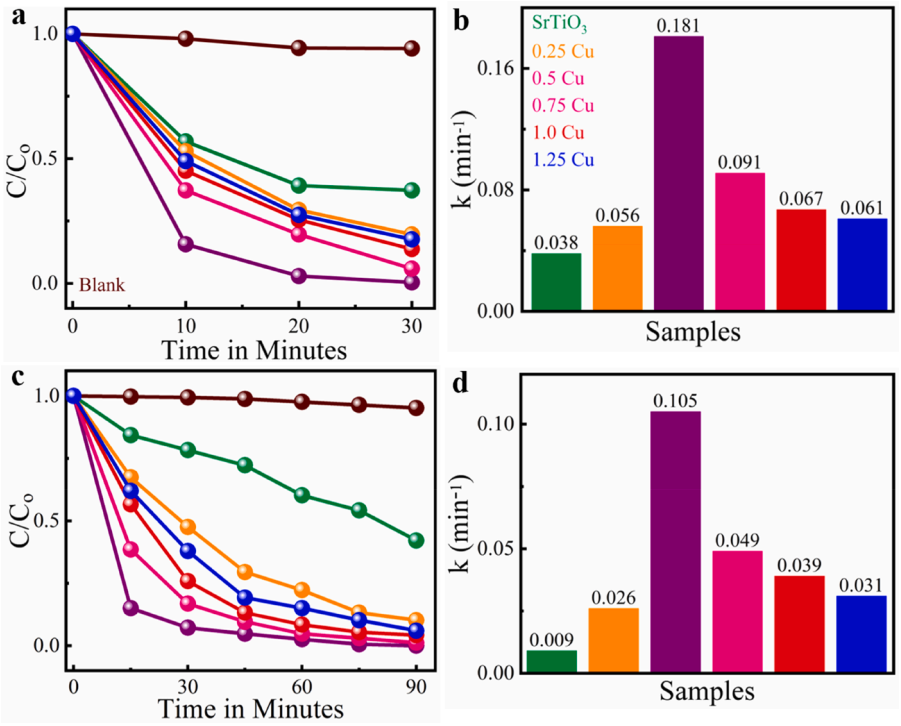

Fig. 3. Photocatalytic (a and b) RB, (c and d) MB dye degradation plots and rate constants in absence of catalyst (blank) and in presence of the synthesized undoped and copper doped $SrTiO_3$ samples.

active species and degradation of the dyes. Higher surface area of the catalyst ensures large number of active sites and in turn enhances the probability of the degradation reaction as it results in easier migration of the active species from the catalyst to the dye molecules (Bantawal et al., 2020).

The UV-DR spectrum of the undoped sample indicates the absorption due to the electronic transition from the O 'p' orbitals to the Ti 'd' orbitals. Unlike the pristine samples, the absorption edges of the doped samples were shifted towards a longer wavelength region confirming the visible light absorption by the doped samples (Fig. 1e). The incorporation of Cu^{2+} into the lattice generates energy levels between the valence and conduction bands leading to decreased band gaps and occurrence of electronic transitions between the donor Cu level and the conduction band as explained in DFT results later. The bandgaps of $SrTiO_3$, 0.25 Cu, 0.5 Cu, 0.75 Cu, 1.0 Cu and 1.25 Cu were estimated to be 3.17 eV, 3.14 eV, 3.04 eV, 3.00 eV, 2.96 eV and 2.91 eV, respectively using Tauc method (Fig. S6) (Bhat et al., 2023). As more and more Cu^{2+}ions get substituted, the width of the donor level increases and comes closer to the conduction band, thus reducing the bandgap progressively. The intensities of the photoluminescent (PL) spectra of photocatalysts reveal the rate of recombination of charge carriers. The photoactivity decreases and the PL intensity rises when there are more emitted photons due to the recombination of excited electrons with holes (Bantawal et al., 2020). When compared to the pristine sample, the fluorescence intensity for the doped samples drastically decreased and the least intensity was observed for the 0.5 Cu sample (Fig. 1f). This illustrates the reduced probability of photoinduced charge recombining in the doped samples. The PL studies show that Cu doping in $SrTiO_3$ reduced the bandgap without elevating the recombination rate, justifying the high performance of the 0.5 Cu as revealed in the subsequent sections.

The electronic structure determined using first principles DFT calculations reveals a direct band gap at Γ point with a band gap estimate of 2.14 eV (Fig. 2a). This underestimation of band gap is typical of DFT based calculations and is well known (Uma et al., 2023; Shenoy and Bhat, 2020; Bhat and Shenoy, 2019). Two indirect band gaps of 1.86 eV and 1.84 eV also occur between M → Γ and R → Γ, respectively. We observe that the valence band edge is purely formed out of 'p' orbitals of oxygen while the conduction band edge is formed of 'd' orbitals of titanium (Fig. 2b) (Shenoy and Bhat, 2021). Substitution of Cu at Sr sites leads to the formation of donor dopant state overlapping with the valence band edge, decreasing the direct band gap to 1.87 eV (Γ point) and indirect band gaps to 1.79 eV (M → Γ) and 1.78 eV (R → Γ). This additional band is very flat in nature formed by the hybridization of 'd' orbitals of copper with 'p' orbitals of oxygen (Fig. 2c and d). At the Fermi level we see a very steep increase in the DOS (Shenoy and Bhat, 2020).

When Cu substitutes Ti, we see that the dopant energy levels rise above the parent valence band edge and reduce the direct band gap to 1.84 eV at Γ point, while both the indirect band gaps see a prominent reduction to 1.44 eV (Fig 2e). Lower band gap is an essential requirement for efficient visible light absorption and in turn for more efficient visible light photocatalysis. The results indicate that higher reduction in the band gap can be achieved when Cu is doped in Ti site than Sr site. This confirms that developing an approach to substitutionally dope Cu into Ti site would be beneficial for the development of visible light active photocatalyst (Uma et al., 2023). The DFT results further support our choice of synthetic technique which directed Cu into Ti site. We observe an interesting feature of generation of deep defect states at 5 eV below the Fermi level in the pDOS when Cu substituted Ti, in addition to the states at the Fermi level due to the hybridization of the orbitals of oxygen (p) and copper (d). Such a feature was absent when Cu substituted Sr. Although the states at the Fermi level are not as intense as the former case here, we see splitting of peaks due to the duplex nature of the bands formed (Fig. 2f).

Aqueous solutions of RB and MB was taken as model dyes to check the photocatalytic activity of the samples (Details in supplementary information). The degradation patterns showed that in the absence of the catalyst, the degradation of the dyes was very feeble, highlighting the importance of the photocatalyst. The degradation plots of RB and MB in Fig. 3a and c indicates that the 0.5 Cu nanocubes degrade the dyes at a higher rate than other samples which is also supported by the BET and PL results. The absorbence of RB and MB decreased with time and 99.6% degradation was observed for RB within 30 min and similarly 100%

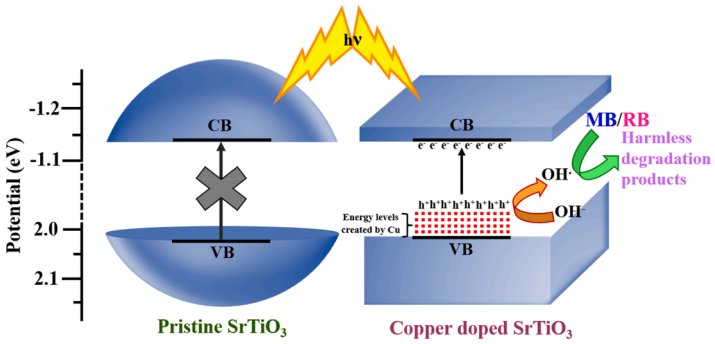

Fig. 4. The mechanism of photocatalytic degradation of RB and MB dyes in presence of undoped and copper doped $SrTiO_3$ catalysts under visible light irradiation.

degradation was observed for MB within 90 min. The 0.5 Cu nanocubes had the highest surface area leading to more active sites and lowest recombination rate aiding the high photocatalytic activity when compared to other samples studied in this work. The kinetics of the photocatalytic degradation of the dyes by $SrTiO_3$ and Cu-doped $SrTiO_3$ is in good agreement with the pseudo first-order rate Eq. (1) given by

$$-ln(C / C_o) = kt \quad (1)$$

where C_o is the initial concentration of dye, C is the concentration of the dye at irradiation time (t) and k is the first-order rate constant. The rate constant k, in turn, is calculated from the slope of the straight line plot of $-\ln(C/C_o)$ versus t (Fig. S7) (Bhat et al., 2023). The trend seen in the rate constants of the photocatalyst was consistent with the PL results (Fig. 3b and d). Thus, photocatalytic experiments clearly point out the superiority of the 0.5 Cu sample in degrading both anionic and cationic dyes. The thermodynamic variables determined indicated that photodegradation in the presence of $SrTiO_3$ and Cu-doped $SrTiO_3$ required less activation energy than without a catalyst (Table S1). The 0.5 Cu sample had the lowest activation energy, enthalpy of activation, and free energy of activation. The lower values demonstrate that the catalyst alters the reaction route, speeding up the reaction (Bantawal et al., 2021). The reaction is endothermic and not spontaneous because the free energy of activation and enthalpy are both positive (Uma et al., 2023). The cyclic stability of the 0.5 Cu sample was measured for both RB and MB dye for 7 cycles and only a trivial reduction in degradation rate was found after each cycle proving the stability of the catalyst (Fig. S8a). Further, the stability of the chemical structure after the photocatalytic reaction was evinced by observing the XRD taken after the reaction. The XRD peaks before and after the reaction were identical revealing no structural changes occurred because of visible light irradiation and photocatalytic degradation reaction (Fig. S8b).

The identification of active species involved in photocatalysis help in explaining the mechanism of dye degradation by the photocatalyst. Trapping experiments were carried out with different scavengers like potassium iodide as a hole scavenger, isopropyl alcohol as a hydroxyl radical (OH) scavenger, and potassium dichromate as a superoxide anion radical ($O_2^{\cdot-}$) scavenger and the result showed that holes and hydroxyl radicals are the active species (Fig. S9) (Girotto et al., 2022; Uma et al., 2023). The low degradation efficiencies of the dyes in the presence of scavengers for holes and hydroxyl radicals confirmed them as active species (Uma et al., 2023). Thus, the mechanism of degradation of dyes can be explained as follows: as material absorbs light energy, the electrons migrate from the valence band to conduction band creating positive holes in the valence band. As the holes have high oxidation capacity, they can directly produce hydroxyl radicals (OH) by interacting with OH^- or H_2O. (Girotto et al., 2022) These active species then degrade the dyes into harmless degradation products due to favourable potential values (Fig. 4) (Uma et al., 2023). The comparison of the activity of the present material with earlier reports indicates the superior activity of the synthesized material (Table S2).

Conclusions

In summary, the synthesized copper doped strontium titanate nanocubes using the one-pot solvothermal method successfully degraded both the anionic and cationic dyes revealing the versatility of the photocatalyst. The copper doping that superseded Ti^{4+} by Cu^{2+} ions altered the electronic structure of $SrTiO_3$ and caused the decrease in the bandgap to the visible region as revealed by the DFT studies. Moreover, the 0.5 Cu sample possessed high surface area, low recombination rate and appropriate band gap to beneficially aid the photocatalysis process. The photocatalytic degradation of 99.6% RB and 100% MB within 30 min and 90 min, respectively in presence of 0.5 Cu nanocubes were quite prodigious indicating its potential application in environmental remediation. Thus, the work provides a promising way for water pollution treatment with renewable solar energy.

Funding information

The financial support was received from Science and Engineering Research Board, Department of Science and Technology, Government of India under SERB Research Scientist scheme.

Declaration of Competing Interest

The authors declare that they have no known competing financial interests or personal relationships that could have appeared to influence the work reported in this paper.

Data availability

Data will be made available on request.

Acknowledgments

The author USS acknowledges the financial support received from Science and Engineering Research Board, Government of India under SRS scheme.

Supplementary materials

Supplementary material associated with this article can be found, in the online version, at doi:10.1016/j.hazadv.2023.100380.

References

Alimohammadi, E., Mahdikhah, V., Alirezazadeh, F., Sheibani, S., Farzin, Y.A., 2023. Plasmonic resonance and type-I heterojunction interface in $SrTiO_3$/CZTS/Ag nanocomposite for enhanced photocatalytic degradation of organic pollutants. Mat. Today Chem. 28, 101378 https://doi.org/10.1016/j.mtchem.2023.101378.

Bantawal, H., Shenoy, U.S., Bhat, D.K., 2018. Tuning photocatalytic activity of $SrTiO_3$ by varying the Sr/Ti ratio: unusual effect of viscosity of synthetic medium. J. Phys. Chem. C 122, 20027–20033. https://doi.org/10.1021/acs.jpcc.8b06514.

Bantawal, H., Sethi, M., Shenoy, U.S., Bhat, D.K., 2019. Porous graphene wrapped $SrTiO_3$ nanocomposite: sr-C bond as an effective coadjutant for high performance photocatalytic degradation of methylene blue. ACS Appl. Nano Mater. 2, 6629–6636. https://doi.org/10.1021/acsanm.9b01513.

Bantawal, H., Shenoy, U.S., Bhat, D.K., 2020. Vanadium-doped $SrTiO_3$ nanocubes: insight into role of vanadium in improving the photocatalytic activity. Appl. Surf. Sci. 513, 145858 https://doi.org/10.1016/j.apsusc.2020.145858.

Bantawal, H., Shenoy, U.S., Bhat, D.K., 2021. Vanadium doped $CaTiO_3$ cuboids: role of vanadium in improving the photocatalytic activity. Nanoscale Adv. 3, 5301–5311. https://doi.org/10.1039/d1na00468a.

Bhat, D.K., Shenoy, U.S., 2019. Zn: a versatile resonant dopant for SnTe thermoelectrics. Mater. Today Phys. 11, 100158 https://doi.org/10.1016/j.mtphys.2019.100158.

Bhat, D.K., Bantawal, H., Shenoy, U.S., 2020. Rhodium doping augments photocatalytic activity of barium titanate: effect of electronic structure engineering. Nanoscale Adv. 2, 5688–5698. https://doi.org/10.1039/d0na00702a.

Bhat, D.K., Bantawal, H., Uma, P.I., Shenoy, U.S., 2023. Enhanced photoresponse and efficient charge transfer in porous graphene-$BaTiO_3$ nanocomposite for high performance photocatalysis. Diam. Relat. Mater. 139, 110312 https://doi.org/10.1016/j.diamond.2023.110312.

Cheng, C., Wang, J., Zhao, Z., Chen, C., Cui, S., Wang, Y., Pan, L., Ni, Y., Lu, C., 2022. S-scheme $SrTiO_3$/porous ZnO derived by pyrolysis of ZIF-8 composite with efficient photocatalytic activity for pollutant degradation. J. Alloy. Compd. 896, 163064 https://doi.org/10.1016/j.jallcom.2021.163064.

Chu, X., Jiang, X., Zhang, H., Wang, C., Huang, F., Sun, X., Li, S., 2022. Microstructure engineering of Al doped $SrTiO_3$/TiO_2 heterostructure nanorod arrays boosting piezo-photocatalytic performances. Adv. Mater. Technol. 7, 2200390 https://doi.org/10.1002/admt.202200390.

Giannozzi, P., Baroni, S., Bonini, N., Calandra, M., Car, R., Cavazzoni, C., Ceresoli, D., Chiarotti, G.L., Cococcioni, M., Dabo, I., Corso, A.D., de Gironcoli, S., Fabris, S., Fratesi, G., Gebauer, R., Gerstmann, U., Gougoussis, C., Kokalj, A., Lazzeri, M., Martin-Samos, L., Marzari, N., Mauri, F., Mazzarello, R., Paolini, S., Pasquarello, A., Paulatto, L., Sbraccia, C., Scandolo, S., Sclauzero, G., Seitsonen, A.P., Smogunov, A., Umari, P., Wentzcovitch, R.M., 2009. Quantum ESPRESSO: a modular and open-source software project for quantum simulations of materials. J. Phys. Condens. Matter 21, 395502. https://doi.org/10.1088/0953-8984/21/39/395502.

Girotto, G.Z., Thill, A.S., Matte, L.P., Vogt, M.A.H., Machado, T.V., Dick, L.F.P., Mesquita, F., Bernardi, F., 2022. Ni/$SrTiO_3$ nanoparticles for photodegradation of methylene blue. ACS Appl. Nano Mater. 5, 13295–13307. https://doi.org/10.1021/acsanm.2c03007.

Jang, H.J., Park, S.J., Yang, J.H., Hong, S.M., Rhee, C.K., Kim, D., Sohn, Y., 2021. Photocatalytic and photoelectrocatalytic properties of Eu(III)-doped perovskite $SrTiO_3$ nanoparticles with dopant level approaches. Mater. Sci. Semicond. Process. 132, 105919 https://doi.org/10.1016/j.mssp.2021.105919.

Kafeshani, M.A., Mahdikhah, V., Sheibani, S., 2022. Facile preparation and modification of $SrTiO_3$ through Ni–Cd co-doping as an efficient visible-light-driven photocatalyst. Opt. Mater. 133, 113080 https://doi.org/10.1016/j.optmat.2022.113080.

Kihoi, S.K., Shenoy, U.S., Kahiu, J.N., Kim, H., Bhat, D.K., Lee, H.S., 2022. Ultra-low lattice thermal conductivity and enhanced mechanical properties of Cu and Sb co-doped SnTe thermoelectric material with a complex microstructure evolution. ACS Sustain. Chem. Eng. 10, 1367–1372. https://doi.org/10.1021/acssuschemeng.1c07817.

Kim, H., Kihoi, S.K., Shenoy, U.S., Kahiu, J.N., Shin, D.H., Bhat, D.K., Lee, H.S., 2023. High Thermoelectric and mechanical performance achieved by hyperconverged electronic structure and low lattice thermal conductivity in GeTe through $CuInTe_2$ alloying. J. Mater. Chem. A 11, 8119–8130. https://doi.org/10.1039/d2ta09280h.

Merrad, S., Abbas, M., Brahimi, R., Trari, M., 2022. Study of congo red removal from aqueous solution by using the deficient perovskite $SrTiO_{3-\delta}$ under solar light. J. Mol. Struct. 1265, 133349 https://doi.org/10.1016/j.molstruc.2022.133349.

Mohamed, M.J.S., Shenoy, U.S., Bhat, D.K., 2018. Novel NRGO-$CoWO_4$-Fe_2O_3 nanocomposite as an efficient catalyst for dye degradation and reduction of 4-nitrophenol. Mater. Chem. Phys. 208, 112–122. https://doi.org/10.1016/j.matchemphys.2018.01.012.

More, G.S., Shivhare, A., Kaur, S.P., Kumar, T.J.D., Srivastava, R., 2022. Catalytic interplay of metal ions (Cu^{2+}, Ni^{2+}, and Fe^{2+}) in MFe_2O_4 inverse spinel catalysts for enhancing the activity and selectivity during selective transfer hydrogenation of furfural into 2-methylfuran. Catal. Sci. Technol. 12, 4857–4870. https://doi.org/10.1039/d2cy00970f.

Nunocha, P., Kaewpanha, M., Bongkarn, T., Phuruangrat, A., Suriwong, T., 2021. A new route to synthesizing La-doped $SrTiO_3$ nanoparticles using the sol-gel auto combustion method and their characterization and photocatalytic application. Mater. Sci. Semicond. Process. 134, 106001 https://doi.org/10.1016/j.mssp.2021.106001.

Nunocha, P., Kaewpanha, M., Bongkarn, T., Eiad-Ua, A., Suriwong, T., 2022. Effect of Nb doping on the structural, optical, and photocatalytic properties of $SrTiO_3$ nanopowder synthesized by sol-gel auto combustion technique. J. Asian Ceram. Soc. 10, 583–596. https://doi.org/10.1080/21870764.2022.2094556.

Ordoñez, M.F., Cerrato, G., Giordana, A., Di Michele, A., Falletta, E., Bianchi, C.L., 2023. One-pot synthesis of Ag-modified $SrTiO_3$: synergistic effect of decoration and doping for highly efficient photocatalytic NO_x degradation under LED. J. Environ. Chem. Eng. 11, 110368 https://doi.org/10.1016/j.jece.2023.110368.

Paul, P.C., Shah, A., Singh, L.R., Mahato, M., Mahato, D.K., 2023. Mn-doped $SrTiO_3$ and $SrTiO_3$–Fe_2O_3 composite perovskites: photocatalytic dye degradation and energy storage application. J. Mater. Sci. Mater. Electron. 34, 1305. https://doi.org/10.1007/s10854-023-10703-4.

Perdew, J.P., Burke, K., Ernzerhof, M., 1996. Generalized gradient approximation made simple. Phys. Rev. Lett. 77, 3865. https://doi.org/10.1103/PhysRevLett.77.3865.

Rahman, Q.I., Ahmad, M., Misra, S.K., Lohani, M., 2012. Efficient degradation of methylene blue dye over highly reactive Cu doped strontium titanate ($SrTiO_3$) nanoparticles photocatalyst under visible light. J. Nanosci. Nanotechnol. 12, 7181–7186. https://doi.org/10.1166/jnn.2012.6494.

Rosy, A., Kalpana, G., 2018. Reduced graphene oxide/strontium titanate heterostructured nanocomposite as sunlight driven photocatalyst for degradation of organic dye pollutants. Curr. Appl. Phys. 18, 1026–1033. https://doi.org/10.1016/j.cap.2018.05.019.

Sadiq, M.M.J., Shenoy, U.S., Bhat, D.K., 2018. Synthesis of $BaWO_4$/NRGO–g-C_3N_4 nanocomposites with excellent multifunctional catalytic performance via microwave approach. Front. Mater. Sci. 12, 247–263. https://doi.org/10.1007/s11706-018-0433-0.

Shenoy, U.S., Bhat, D.K., 2020a. Enhanced thermoelectric properties of vanadium doped $SrTiO_3$: a resonant dopant approach. J. Alloy. Compd. 832, 154958 https://doi.org/10.1016/j.jallcom.2020.154958.

Shenoy, U.S., Bhat, D.K., 2020b. Vanadium doped $BaTiO_3$ as high performance thermoelectric material: role of electronic structure engineering. Mater. Today Chem. 18, 100384 https://doi.org/10.1016/j.mtchem.2020.100384.

Shenoy, U.S., Bhat, D.K., 2021. Electronic structure engineering of $SrTiO_3$ via rhodium doping: a DFT study. J. Phys. Chem. Solids 148, 109708. https://doi.org/10.1016/j.jpcs.2020.109708.

Shenoy, U.S., Bantawal, H., Bhat, D.K., 2018. Band engineering of $SrTiO_3$: effect of synthetic technique and site occupancy of doped rhodium. J. Phys. Chem. C 122, 27567–27574. https://doi.org/10.1021/acs.jpcc.8b10083.

Sohrabian, M., Mahdikhah, V., Alimohammadi, E., Sheibani, S., 2023. Improved photocatalytic performance of $SrTiO_3$ through a Z-scheme polymeric-perovskite heterojunction with g-C_3N_4 and plasmonic resonance of Ag mediator. Appl. Surf. Sci. 618, 156682 https://doi.org/10.1016/j.apsusc.2023.156682.

Song, Y.X., Ma, W.Q., Chen, J.J., Xu, J., Mao, Z.Y., Wang, D.J., 2021. Photocatalytic activity of perovskite $SrTiO_3$ catalysts doped with variable rare earth ions. Rare Met. 40, 1077–1085. https://doi.org/10.1007/s12598-020-01674-0.

Sun, Y., Xia, Y., 2002. Shape-controlled synthesis of gold and silver nanoparticles. Science 298, 2176–2179. https://doi.org/10.1126/science.1077229.

Uma, P.I., Shenoy, U.S., Bhat, D.K., 2023a. Electronic structure engineering of $BaTiO_3$ cuboctahedrons by doping copper to enhance the photocatalytic activity for environmental remediation. J. Alloy. Compd. 948, 169600 https://doi.org/10.1016/j.jallcom.2023.169600.

Uma, P.I., Shenoy, S.U., Bhat, D.K., 2023b. Nanocubic copper doped $SrTiO_3$ for photoreduction of Cr (VI) and photodegradation of methyl violet. ACS Appl. Nano Mater. 6, 16798–16804. https://doi.org/10.1021/acsanm.3c02997.

Uma, P.I., Shenoy, U.S., Bhat, D.K., 2023c. Doped $BaTiO_3$ cuboctahedral nanoparticles: role of copper in photocatalytic degradation of dyes. Appl. Surf. Sci. Adv. 15, 100408 https://doi.org/10.1016/j.apsadv.2023.100408.

Wang, N., Li, Z.J., Gao, H., Li, R., Xu, X.F., Li, T., Long, Y.Z., Zhang, H.D., 2023. Enhanced visible-photocatalytic activities in strong acids and strong alkalis of flexible iron-$SrTiO_3$ nanofibrous membranes. Langmuir 39, 6885–6895. https://doi.org/10.1021/acs.langmuir.3c00506.

Xu, Y., Liang, Y., He, Q., Xu, R., Chen, D., Xu, X., Hu, H., 2023. Review of doping $SrTiO_3$ for photocatalytic applications. Bull. Mater. Sci. 46 (6) https://doi.org/10.1007/s12034-022-02826-x.

Zhang, Z., Chen, R., Wang, L., Chen, X., Ding, J., Zhang, J., Wan, H., Guan, G., 2023. Synergistic effect of Cu^{2+} and Cu^{+} in $SrTiO_3$ nanofibers promotes the photocatalytic reduction of CO_2 to methanol. Appl. Surf. Sci. 609, 155297 https://doi.org/10.1016/j.apsusc.2022.155297.

Zhu, J., Zhang, Y., Shen, L., Li, J., Li, L., Zhang, F., Zhang, Y., 2022. Hydrothermal synthesis of Nb^{5+}-doped $SrTiO_3$ mesoporous nanospheres with greater photocatalytic efficiency for Cr(VI) reduction. Powder Technol. 410, 117886 https://doi.org/10.1016/j.powtec.2022.117886.